
On the relationship between Dropout and Equiangular Tight Frames

Dor Bank
Tel Aviv University

Raja Giryes
Tel Aviv University

Abstract

Dropout is a popular regularization technique in neural networks. Yet, the reason for its success is still not fully understood. This paper provides a new interpretation of Dropout from a frame theory perspective. This leads to a novel regularization technique for neural networks that minimizes the cross-correlation between filters in the network. We demonstrate its applicability in convolutional and fully connected layers in both feed-forward and recurrent networks.

1 Introduction

Deep neural networks are powerful computational models that are being used extensively for solving problems in computer vision, speech recognition, natural language processing, and many other areas [Krizhevsky et al., 2012, Hinton et al., 2012a, Kim, 2014, Zhang et al., 2016, Voulodimos et al., 2018]. The parameters of these models are learned from a given training set. Thus, regularization strategies for preventing overfitting are needed. Several of them have been developed in the recent years [Goodfellow et al., 2016, Kukaka et al., 2017].

One of the most popular strategies is *Dropout*, which randomly drops hidden nodes along with their connections at training time [Hinton et al., 2012b, Srivastava et al., 2014]. During training, in each batch, feature detectors are multiplied by a Bernoulli(p) variable, which causes them to nullify with a probability of $q = 1 - p$. The remaining weights are trained by back-propagation regularly. At test time, all weights are multiplied by p to sustain the overall norm.

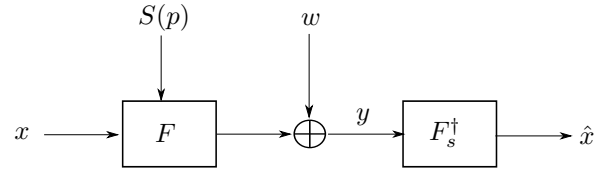


Figure 1: Signal encoding in an analog channel with a decoding scheme that performs least squares based inversion. $x, \hat{x} \in \mathbb{R}^m$ are the input and reconstructed signals respectively, $y, w \in \mathbb{R}^{p \cdot n}$ are the sampled noisy signal and the noise added to it, and $S(p)$ is a sampling pattern that erases a fraction of p entries from xF . Notice the similarity to a denoising autoencoder with a dropout regularization and an additive noise: The encoder A is the linear operation F , the sampling operation $S(p)$ is equivalent to dropout, and the decoder B calculates the pseudo inverse F_s^\dagger , which is the least squares solution to recover the input from the representation y given the sampled encoder F_s . The optimal F in this case is shown to be an ETF, which leads to a new understanding of Dropout and an ETF based regularization technique for neural networks.

Though very useful, Dropouts explicit regularization is not fully understood yet. Such understanding is needed to exploit the full potential of Dropout, and to deepen our knowledge in neural networks.

In this work, we approach Dropout from a signal processing and information theory perspective. We draw a relationship between Dropout and the problem of signal recovery from erasures in the analog domain (see Figure 1). In this “analog coding” problem, a signal passes through an encoder A and then disrupted by an additive noise and part of its values are nullified. Once received, it is recovered by passing through a decoder B . The goal is to find the pair (A, B) , which recovers the input signal with a minimal ℓ_2 error.

To draw the connection to dropout, we make the following steps. First, we examine a specific case, where the encoding A is performed by a (linear) matrix mul-

tiplication F , and the recovery is done by solving the linear least squares problem with the given measurements and $F_{S(p)}$, the subset of columns from the matrix F corresponding to the kept measurements. It has been suggested in a recent work that an equiangular tight frame (ETF), a matrix whose columns have the smallest possible correlation in absolute value between each other, is the best choice for such cases.

Next, we draw a relationship to autoencoders (briefly illustrated in Figure 1). An autoencoder is a type of a neural network used to learn an efficient data representation in an unsupervised manner. It is decomposed of two parts, the first that encodes the data and the second that decodes it from the learned representation. Considering an autoencoder with a linear operator at the encoder and a dropout regularization with it, we get a very similar structure to the analog coding problem. Thus, if the decoder solves the least squares solution, then an ETF is likely to be a global minimum in the optimization of the encoder.

Last, we notice the representation learned by autoencoders may be used for classification, e.g., in semi-supervised learning setups, where the learned encoder serves as a feature extractor. This leads us to the conjecture that promoting structure of an ETF in some layers of the network might turn useful for classification tasks as well.

We support our claim by experiments done on various data-sets for image classification and word level prediction. We measure the effect of the ETF regularization when used as a sole regularizer, and when combined with Dropout. For fully connected (FC) layers, we promote an ETF structure for the weight matrix directly by reducing the correlation between its rows. We demonstrate this regularization for both feed-forward and recurrent (LSTM) networks. For convolutional layers that, we do not use their corresponding Toeplitz matrix. Instead, for simplicity, the coherence between the convolution kernels is minimized.

2 Related work

Other regularization techniques. Many regularization techniques other than dropout have been proposed for neural networks [Goodfellow et al., 2016, Kukaka et al., 2017]. We briefly mention some of them. Batch Normalization [Ioffe and Szegedy, 2015] aims at normalizing the variance of the features at a given layer of the network. Another example is DropConnect [Wan et al., 2013], which is a variation of Dropout, where the weights are nullified with probability q instead of the features. Thus, all the features participate in each batch while only p of the weights (chosen randomly at each forward pass) are used.

Weight decay [Krogh and Hertz, 1992], is a regularization that minimizes the ℓ_2 norm of the layer weights, intentionally reducing their flexibility. Replacing the ℓ_2 norm with ℓ_1 has been also explored [Scardapane et al., 2017, Zhang et al., 2015]. While the latter induces sparse weight matrices, it is harder to optimize, yielding weight decay a more commonly used method. Another alternative to weight decay is Jacobian regularization. It has been proposed for autoencoders in [Rifai et al., 2011], and in [Sokolic et al., 2017] suggested for general neural networks showing that it increases the input margin in them, and thus improving their performance.

Theoretical foundation for Dropout. After the success of Dropout, an extensive research was performed to understand the theory behind it. Baldi et al. introduced a general formalism for studying Dropout in neural networks with the sigmoid activation function and proved that the weighted geometric mean of all of the sub-networks associated with the retained units at each iteration can be computed with a single forward pass [Baldi and Sadowski, 2013, P. Baldi, 2014]. Wager et al. analyzed Dropout applied to the logistic loss for generalized linear models [Wager et al., 2013]. The work in [Helmbold and Long, 2015] discussed the mathematical properties of Dropout and derived a sufficient condition to guarantee a unique minimizer for a loss function in which Dropout is used.

Wager et al. have shown that under a generative Poisson topic model with long documents, Dropout training improves the exponent in the generalization bound for empirical risk minimization [Wager et al., 2014]. Cavazza et al. have discussed the equivalence between Dropout and a fully deterministic model for Matrix Factorization in which the factors are regularized by the sum of the product of the squared Euclidean norms of the columns of the matrix [Cavazza et al., 2018].

Mianjy et al. study the implicit bias of Dropout [Mianjy et al., 2018]. They show that for some settings, applying Dropout is equivalent to the square of the convex Path-Regularization [Neyshabur et al., 2015], which is the square-root summation over all paths in the network, where in each path the squared weights product is calculated. It is shown that for a linear autoencoder with an encoder matrix A and a decoder matrix B , if (A, B) is a global minimum, then $\forall i, \|A_i\| \|B_i\| = \|A_1\| \|B_1\|$, where A_i and B_i are the i th columns in A and B respectively.

Use of autoencoders for classification. Autoencoders have been first introduced in [Rumelhart et al., 1986] as a neural network that is trained to reconstruct its input. Their main

purpose is learning in an unsupervised manner an “informative” representation of the data that can be used for clustering. The problem, as formally defined in [Baldi, 2012], is to learn the functions $A : \mathbb{R}^n \rightarrow \mathbb{R}^p$ (encoder) and $B : \mathbb{R}^p \rightarrow \mathbb{R}^n$ (decoder) that satisfy

$$\operatorname{argmin}_{A,B} E[\Delta(x, B \circ A(x))], \quad (1)$$

where Δ is an arbitrary distortion function, which is set to be the ℓ_2 -norm in our case, and E is the expectation over the distribution of x .

In the most popular form of autoencoders, A and B are neural networks [Ranzato et al., 2007]. In the special case that A and B are linear operations, we get a linear autoencoder [Baldi and Hornik, 1989].

Since in training one may just get the identity operator for A and B , which keeps the achieved representation the same as the input, some additional regularization is required. One option is to make the dimension of the representation smaller than the input. Another option is using denoising autoencoders [Vincent et al., 2008]. In these architectures, the input is disrupted by some noise (e.g., additive white Gaussian noise or erasures using Dropout) and the encoder is expected to reconstruct the clean version of the input.

Another major improvement in the representation capabilities of autoencoders has been achieved by the variational autoencoders [Kingma and Welling, 2013]. These encode the input to latent variables, which represent a distribution, and decode it by learning the posterior probability of the output from it.

Autoencoders may be trained end-to-end or gradually layer by layer. In the latter case, they are “stacked” together, which leads to a deeper encoder. In [Masci et al., 2011], this is done with convolutional autoencoders, and in [Vincent et al., 2010] with denoising ones.

Autoencoders are also used for classification by using the encoder as a feature extractor and “plugging” it into a classification network. This is mainly done in the semi-supervised learning setup. First, the autoencoders are trained as described above in an unsupervised way. Then (or in parallel), the encoder is used as the first part of a classification network, and its weights may be fine tuned or not vary during training [Kingma and Welling, 2013]. Notice that different types of autoencoders may be mixed to form new ones, as in [Pu et al., 2016], which uses them for classification, captioning, and unsupervised learning.

We shall use hereafter this relationship between autoencoders and classification neural networks to transfer a regularization that is proven to be helpful in the encoder-decoder setup to the classification case.

3 Method

3.1 Equiangular tight frames

Frames, or over-complete bases, are $m \times n$ matrices with rank m , where $n > m$. They are widely used in various applications of communication, signal processing, and harmonic analysis [Bodmann et al., 2008, Casazza et al., 2008, Christensen, 2003, Han and Larson, 2000]. For example, they are often used for sampling techniques to analyze and digitize signals and images when they are represented as vectors or functions in a Hilbert space [Eldar, 2015]. There is also a great interest in finding frames with favorable properties that hold for random subsets of their columns [Rupf and Massey, 2006].

One popular type of frames is tight frames. A frame F of dimensions $m \times n$ is a tight frame iff $FF^T = c \cdot I_m$ for some constant c . In [Cotfas and Gazeau, 2010], they have been shown to be useful for quantization.

The Gram matrix of a frame $G_F = F^T F$ contains outside its diagonal the cross-correlation values between the columns of the frame F , i.e., $G_{i,j}$ contains the cross-correlation value between the i th and j th columns of F . The Welch bound [Welch, 1974] provides a universal lower bound on the mean and maximal absolute value of the cross-correlations between the frame vectors. A frame that achieves the Welch lower bound on the maximal absolute cross-correlation value is known as an equiangular tight frame (ETF). Notice that ETFs are a sub-group of tight frames. The gram matrix G_{ETF} of a $m \times n$ ETF satisfies:

$$(G_{ETF})_{i,j} = \begin{cases} 1 & i = j \\ \frac{n-m}{(n-1)m} & \text{else.} \end{cases} \quad (2)$$

Intuitively, its n vectors are spread uniformly across an m dimensional space with an angle of $\theta = \arccos \sqrt{\frac{n-m}{(n-1)m}}$ between them. The maximal off-diagonal value in the gram matrix is denoted the mutual coherence [Donoho and Elad, 2003] or simply the coherence value.

3.2 Signal reconstruction from a frame representation with erasures

We turn now to define our problem setup illustrated in Figure 1. Consider the signal vector $x \in \mathbb{R}^m$ and a frame F . First, the vector is encoded by F , i.e., yielding xF , which is then transmitted in an analog channel. In the channel, part of the values are nullified with probability p , and then the remaining values are disrupted by an additive white Gaussian noise (AWGN).

Notice that nullifying the values in x^F with probability p is equivalent to removing columns from F with probability p and then multiplying it with x . Denote by $S(p)$ the pattern that defines which vectors of F are used, with respect to the probability p , and by F_s the sub-matrix of F with the vectors corresponding to $S(p)$. Then the resulted vector after the addition of the AWGN w is defined as

$$y = xF_s + w. \quad (3)$$

In order to recover the input from y , one may use the least square solution

$$\hat{x} = \operatorname{argmin}_{\hat{x}} \|y - \hat{x}F_s\|_2^2 = yF_s^\dagger, \quad (4)$$

where F_s^\dagger is the pseudo-inverse of F_s . Thus, if one wishes to optimize F for minimizing the reconstruction error in the ℓ_2 sense, the target objective is:

$$\operatorname{argmin}_F E \|x - \hat{x}\|_2 = \operatorname{argmin}_F E \|x - yF_s^\dagger\|_2. \quad (5)$$

A number of works have studied the problem of reconstruction from erasures (see for example [Casazza and Kovačević, 2003, Bodmann and Paulsen, 2005, Casazza and Kutyniok, 2008, Larson and Scholze, 2015]). For our specific problem setup, it is claimed in [Haikin and Zamir, 2016] that frames whose random subsets resemble the classical MANOVA (also known as Jacobi) random matrix ensemble, minimizes Eq. (5) in the high SNR regime assuming the inputs are i.i.d Gaussian distributed.

More recently it has been shown in [Haikin et al., 2017] that the subsets of ETF matrices have MANOVA distribution, and for large n , they converge to the Wachter’s MANOVA spectral distribution [Wachter, 1980]. In a following work [Haikin et al., 2018], the relationship between the MANOVA distribution and ETFs has been further supported by showing similarity between the moments of the MANOVA distribution and the ones of the ETF. The d -th moment of a random subset in F is defined as

$$m_d \triangleq \frac{1}{n} E[\operatorname{Tr}((FPF^T)^d)], \quad (6)$$

where $\operatorname{Tr}(\cdot)$ is the trace operator and P is a diagonal matrix with independent Bernoulli(p) elements on its diagonal.

It has been proven for $d = 2, 3, 4$ that these moments are lower bounded by the moments of matrices with the Wachter’s classical MANOVA distribution, plus a vanishing term (as n goes to infinity with $\frac{m}{n}$ held constant). The bound is proven to hold with equality for ETFs, where in the case of $d = 4$ it is shown that it

holds only for ETFs. This leads us to assume that the subsets of ETF matrices indeed have MANOVA distribution, and by thus it is conjectured that ETFs are indeed the global minimum for the settings of Eq. (5).

3.3 The relationship between Dropout and ETF

Notice the great resemblance between a denoising autoencoder and the analog coding problem, as illustrated in Figure 1. Given the above information, in the case that the encoder is linear and the decoder calculates the least squares solution, we believe that the global minimum of training with Gaussian distributed data and noise, and Dropout on the encoder should be an ETF for the encoder (or very close to it if the setting slightly changes).

To examine further the relationship between Dropout and ETFs we set an experiment, with an autoencoder that has a similar structure to the analog coding problem setup described in Section 3.2. The encoder A in this network is a linear one, represented by a randomly initialized matrix. Specifically, we use a matrix A of size 75×150 .

For the decoder we do not use A_s^\dagger since it is hard to calculate its derivative with respect to A in the network training. Instead, we use the fact that the pseudo inverse is the least squares solution and perform ten iterations of gradient descent $\hat{x}^{i+1} = \hat{x}^i - \mu A_s^T (A_s \hat{x}^i - y)$, where $\hat{x} = \hat{x}^9$ and $x = \hat{x}^0$. The learning rate μ is the inverse of the largest eigenvalue of the gram matrix $A_s^T A_s$ as in [LeCun et al., 1993]. For getting the sample pattern $S(p)$ we simply apply Dropout on the encoder.

The input signals are generated as i.i.d. Gaussian vectors with a standard deviation of 1 and the noise is generated with the same distribution but with a standard deviation of 0.001.

As can be seen in Figure 2 (for the case $\beta = 0$) the resulted coherence in the matrix A is very far from the Welch bound. We conjecture that this is mainly because the problem is non-convex. To alleviate this, we have added a regularization in the form of

$$\beta \cdot \max(|A^T A| - G_{ETF}), \quad (7)$$

where $|\cdot|$ is an element-wise absolute value, and β is the regularization coefficient. Notice that this term encourages getting an ETF-like structure. We train the autoencoder with this new regularization with several values of β . Figure 2 shows that until a certain value, both the error and the coherence diminish as β increases. This demonstrates that adding this term indeed helps in improving the convergence of the encoding frame to the desired "global minimum".

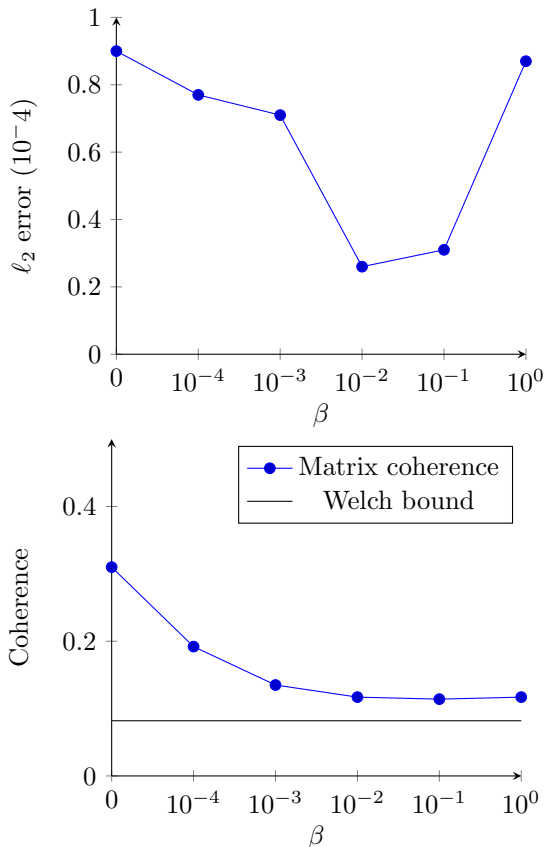


Figure 2: Top: Average ℓ_2 reconstruction error vs. the ETF regularization parameter β . Bottom: Matrix coherence vs. the ETF regularization parameter β .

Notice that we get that for big values of β , both the loss and the coherence values increase although our regularization promotes directly an ETF structure. Also in this case, we conjecture that this is due to the fact that the problem is non-convex. Moreover, notice that there is also a minor difference in the reconstruction setup that may also have some effect (as the decoder of the network uses an approximation of the least squares solution).

Recalling the setting of Section 3.2, notice that the encoding part is exactly equivalent to a FC layer in a neural network, where the frame F plays the roll of the weight matrix, and the nullification with probability p acts as Dropout. Though the specific setup discussed here is more relevant to autoencoders, we believe that the new understandings about Dropout may be carried also to more general neural networks. Inspired by the usage of autoencoders for classification, we conjecture that although ETFs are introduced here for signal recovery, they can be also used to enhance the Dropout regularization also in other networks training, e.g. for classification.

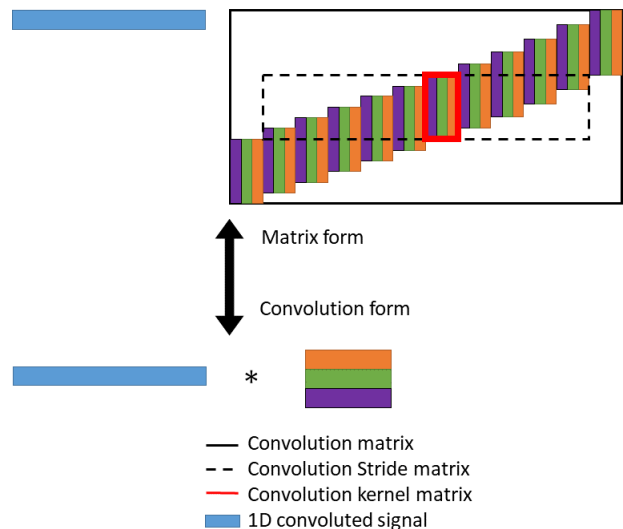


Figure 3: An illustration in the 1D case of the equivalence between a convolution with three kernels and a multiplication with the equivalent Toeplitz matrix. Notice that the coherence of the convolution Toeplitz matrix is the same as the coherence of the smaller convolution stride matrix (marked by dashed lines).

3.4 Coherence as a mean to promote an ETF-like structure

Since there are infinitely many ETFs, we do not want to regularize a layer towards a specific one. Moreover, we do not always have an ETF construction for every combination of m and n . Yet, the structure of the Gram matrix is easily accessible and is the same for all ETFs that have the same value of m and n .

For these reasons, and the ones specified at 3.3, we adopt the "ETF similarity" term presented in Eq. (7) also for general neural networks and in particular to ones for classification. Notice that in the case where $m > n$, all vectors can be independent, and we penalize the distance from I_m , which is the same as reducing the absolute values of the off-diagonal entries of $A^T A$.

To apply our regularization on convolutional layers, we may use their corresponding convolution Toeplitz matrix as illustrated in Figure 3. Notice that the coherence of the convolution Toeplitz matrix is the same as the coherence of the smaller convolution stride matrix (marked by dashed lines) and thus, we apply the regularization directly on the stride convolution matrix. Yet, for simplicity, we just regularize the coherence between the convolution kernels (the matrix marked in red in Figure 3), which is the central part of the stride matrix. In the multi-dimensional case, each kernel is column-stacked and treated as a column vector in the

regularized matrix.

In a LSTM cell, we have four different FC gates: One to create a new state vector; one to create a *forget* vector, which decides how much to keep from the old state; One for an *input* vector, which decides how much to keep from the new state; and one for the cell’s *output*. We promote ETF-like matrices on each one of them separately, since we do not want to impose low coherence between the vectors of the different FC layers. We may want that the same filter will be used in the different gates.

Interestingly, our proposed coherence based regularization technique may also be motivated by the sparse coding theory, where it is well known that it is easier to recover the sparse representation of a vector from a matrix that has a low coherence [Donoho and Elad, 2003, Elad, 2007]. In a recent work, it has been shown that the layers of a convolutional neural network may be viewed as stages for reconstructing the sparse representation of the input [Papayan et al., 2018]. Moreover, recovery guarantees have been developed based on the coherence showing that a smaller coherence leads to better reconstruction of the sparse representation of the input by the network [Papayan et al., 2017]. While that work focuses mainly on convolutional layers, it definitely provides another motivation for our new regularization technique. Especially that in classical sparse coding the coherence is also used with regular matrices (equivalent to the weights in the FC layers).

Practically, there are few ways for promoting a matrix A to be an ETF-like, i.e., making its coherence as small as possible. We focus on three of them: minimizing the sum of squares of $|A^T A| - G_{ETF}$, its sum of absolute values and its maximal value, which is equivalent to minimizing the coherence of A as in (7). Notice that minimizing the sum of absolute values is similar to the approach used in [Elad, 2007] for minimizing the coherence in a dictionary by reducing the average absolute value of the cross-correlations between its columns. Another approach proposed in [Duarte-Carvajalino and Sapiro, 2009] relies on a spectral decomposition of A . Though it is shown to be more effective than the one in [Elad, 2007], it is too computationally demanding for using it with a neural network training and thus we focus just on techniques that minimize the coherence directly.

We compare the three regularization options above on a classification task performed on the Fashion MNIST dataset. We regularize the FC layer in a LeNet5 type network (the exact experiment settings are detailed in Section 4). Table 1 presents the classification accuracy on the training set. We select for each regularization

Table 1: Ablation study of the ETF optimization criterion on LeNet5 FC layer with Fashion MNIST.

Regularization	Accuracy
None	88.36%
ETF max (ℓ_∞)	90.89%
ETF sum (ℓ_1)	88.89%
ETF squared (ℓ_2)	89.22%

strategy its own optimal parameter β . This table suggests that minimizing the coherence directly, i.e. the maximal value in $|A^T A| - G_{ETF}$ as appears in Eq. (7), should be the preferred option.

4 Experiments

We evaluate our method apart of and on top of Dropout. In order to isolate the effect of the two methods, no other regularization techniques are used. We demonstrate our proposed strategy on FC layers, convolutional layers, and LSTM based recurrent neural networks (RNNs). Four known datasets are used with their appropriate architectures.

Fashion MNIST. The Fashion MNIST [Xiao et al., 2017] is a dataset similar to MNIST but with fashion related classes that are harder to classify compared to the standard MNIST. It is composed of 60,000 examples as the train set, and 10,000 as the test set. Each example is a 28×28 grayscale image, associated with a label from 10 fashion related classes.

The architecture we used is based on LeNet5, and was changed a bit to examine a case where $m > n$. The FC layers were changed from $400 \rightarrow 120 \rightarrow 84 \rightarrow 10$ to $400 \rightarrow 800 \rightarrow 10$. For the FC layers, the ETF parameter was set to 100, and the Dropout to 0.5. For the convolutional layers, when used as a sole regularizer, the ETF parameter was increased to 1000. The batch size was 128 and the score was taken as the best one in 400 epochs. The optimizer used was ADAM with a learning rate that diminished from 10^{-3} to 10^{-5} .

CIFAR-10. The CIFAR-10 dataset is composed of 10 classes of natural images with 50,000 training images, and 10,000 testing images. Each image is an RGB image of size 32×32 .

The architecture is based on a variant of Lenet5 for this data set. It involves $5 \times 5 \times 32$ and $5 \times 5 \times 64$ convolution layers with 2×2 max pooling, followed by two FC layers of $1600 \rightarrow 1024 \rightarrow 10$. For the FC layers, the ETF parameter was set to 10 when it is the sole regularizer, and to 1 when combined with Dropout.

For the convolutional layers, it was set to 10. The Dropout parameter was 0.5. The batch size was 128 and the score was taken as the best one in 300 epochs. The optimizer used was Nesterov Momentum with a momentum parameter of 0.9 and a learning rate that diminished from 10^{-2} to 10^{-3} .

Tiny ImageNet. The Tiny Imagenet dataset is composed of 200 classes of natural images with 500 training examples per class, and 10,000 images for validation. Each image is an RGB image of size 64×64 . It is tested by top-1 and top-5 accuracy.

The architecture we use is an adaptation of the VGG-16 model [Simonian and Zisserman, 2015] to the Tiny Imagenet dataset [VGG, 2017]. It consists of ten 3×3 convolution layers, separated to four parts: two layers with 64 feature maps, two with 128, three with 256, and three with 512. All parts are separated by a 2×2 max pool, and after the last convolutional layer there is no pooling but FC layers of $25088 \rightarrow 4096 \rightarrow 2048 \rightarrow 200$.

For the FC layers, the ETF parameter was set to 10 when is the sole regularizer, and to 1 when combined with Dropout. For convolutional layers, It was set to 1. The Dropout parameter was 0.5. The batch size was 64 and the score was taken as the best one in 50 epochs. The optimizer used was Nesterov Momentum with a momentum parameter of 0.9 and a learning rate that diminished from 10^{-2} by a factor of 5 when validation top-1 accuracy ceased increasing.

Penn Tree Bank. We performed word level prediction experiments on the Penn Tree Bank data set [Marcus et al., 1993]. It consists of 929,000 training words, 73,000 validation words, and 82,000 test words. The vocabulary has 10,000 words. In this data set, we measure the results by the attained perplexity, which we aim at reducing.

The architecture is as described in [Zaremba et al., 2014]. Two models are considered, where all of them involve LSTMs with two-layer, which are unrolled for 35 steps. The *small* model includes 200 hidden units, and the *medium* includes 650.

Small model parameters: When used as a sole regularizer, the ETF parameter was set to 1, and when combined with Dropout, to 0.1. The Dropout was set to 0.75. The score was taken as the best one in 30 epochs on the validation set. The optimizer used was Gradient Decent and the learning rate diminished from 1 by a factor of 0.7.

Medium model parameters: When used as a sole regularizer, the ETF parameter was set to 50, and when

Table 2: Fashion MNIST - FC layer regularization

Regularization	Accuracy
None	88.36%
Dropout	90.16%
ETF	90.89%
Dropout+ETF	91.91%

Table 3: CIFAR-10 - FC layer regularization

Regularization	Accuracy
None	84.41%
Dropout	86.16%
ETF	86.14%
Dropout + ETF	86.94%

combined with Dropout, to 1. The Dropout was set to 0.5. The score was taken as the best one in 45 epochs on the validation set. The optimizer used was Gradient Decent and the learning rate diminished from 1 by a factor of 0.8.

4.1 Fully connected layers

We start by applying our ETF regularization on the FC layers on the three image classification data sets: Fashion MNIST (Table 2), CIFAR-10 (Table 3) and Tiny ImageNet (Table 4).

As can be seen in tables 2, 3 and 4, The ETF regularization improves the test accuracy, with and without Dropout. Notice that it always improves the results of dropout when combined together with it and that on the Fashion MNIST data it got better performance also when it was used alone.

4.2 Convolutional layers

Next, we apply our ETF regularization on the convolutional layers. For Fashion MNIST (Table 5) and CIFAR 10 (Table 6), we applied it on the second convolutional layer - right before the FC ones. For Tiny ImageNet (Table 7), we applied it on the last three convolution layers - the ones with feature maps of size

Table 4: Tiny ImageNet - FC layer regularization

Regularization	top-1	top-5
None	39.92%	65.29%
Dropout	48.35%	73.13%
ETF	44.21%	69.34%
Dropout + ETF	49.78%	73.55%

Table 5: Fashion MNIST - conv layer regularization

Regularization	Accuracy
None	88.36%
Dropout	91.14%
ETF	90.30%
Dropout+ETF	91.58%

Table 6: CIFAR-10 - conv layer regularization

Regularization	Accuracy
None	84.41%
Dropout	85.75 %
ETF	85.15%
Dropout + ETF	86.36%

512. Dropout in all cases is applied once after the convolutional layers. In the case of the first two networks it is applied after the pooling operation that follows the convolutions (since this gave better performance with Dropout).

It can be observed that the ETF regularization has less effect on the convolutional layers compared to the FC ones, both when applied with and without Dropout. We conjecture that for classification tasks, the kernels of the different channels have already lower coherence than the columns of a FC weight matrix. It might be also that a regularization of the coherence of the stride matrix may lead to better results.

4.3 Recurrent network

Lastly, we apply our ETF regularization on LSTM cells. We test it for both the small sized model (Table 8), and the medium sized one (Table 9).

Notice that in this case we also see the positive effect of the ETF regularization mainly when combined with the Dropout regularization. When applied alone, the effect of the ETF regularization is weaker in the medium model compared to the small one though it always leads to improvement. We believe that this difference should be further investigated.

Table 7: Tiny ImageNet - conv layer regularization

Regularization	top-1	top-5
None	39.92%	65.29%
Dropout	43.44%	69.03%
ETF	42.13%	67.05%
Dropout + ETF	45.55%	69.80%

Table 8: Penn Tree Bank - small model

Regularization	Val Perp.	Test Perp.
None	121.39	115.91
Dropout	98.260	93.927
ETF	104.425	99.398
Dropout + ETF	93.998	90.139

Table 9: Penn Tree Bank - medium model

Regularization	Val Perp.	Test Perp.
None	123.012	122.853
Dropout	87.059	83.059
ETF	115.868	111.956
Dropout + ETF	85.267	81.646

5 Conclusions

This work provides a novel interpretation of the role of Dropout by bringing together two, similar but "unacquainted", research fields, namely, deep learning and frame theory. This combination has led to the understanding that Dropout promotes an ETF structure when applied on a linear encoder in an autoencoder model. We have shown that adding a regularization that encourages an ETF structure improves the performance in these networks. The fact that in semi-supervised learning, the encoder also serves many times as a feature extractor for classification tasks, has led us to the usage of this ETF regularization also in standard neural networks, e.g., for classification, along with Dropout. This combination has shown improvement in many tasks and network types.

It appears that the study of frames can help to gain a better understanding of the Dropout regularization. We believe that this paper makes the first steps in this direction by studying the optimal frame created by Dropout in an autoencoder architecture that has a linear encoder. The improvement demonstrated in this work by the ETF regularization together with Dropout, for various tasks such as classification, suggests that the role of ETF in neural network optimization should be more deeply analyzed in these contexts.

Acknowledgments

We thank Prof. Ram Zamir and Marina Haikin for fruitful discussion and for introducing us to the analog coding setup. This work is supported by the ERC-STG SPADE grant.

References

- [VGG, 2017] (2017). VGG code for tiny imagenet. https://github.com/pat-coady/tiny_imagenet.
- [Baldi, 2012] Baldi, P. (2012). Autoencoders, unsupervised learning, and deep architectures. In Guyon, I., Dror, G., Lemaire, V., Taylor, G., and Silver, D., editors, *Proceedings of ICML Workshop on Unsupervised and Transfer Learning*, volume 27 of *Proceedings of Machine Learning Research*, pages 37–49, Bellevue, Washington, USA. PMLR.
- [Baldi and Hornik, 1989] Baldi, P. and Hornik, K. (1989). Neural networks and principal component analysis: Learning from examples without local minima. *Neural Netw.*, 2(1):53–58.
- [Baldi and Sadowski, 2013] Baldi, P. and Sadowski, P. J. (2013). Understanding dropout. In Burges, C. J. C., Bottou, L., Welling, M., Ghahramani, Z., and Weinberger, K. Q., editors, *Advances in Neural Information Processing Systems 26*, pages 2814–2822. Curran Associates, Inc.
- [Bodmann et al., 2008] Bodmann, B. G., Casazza, P., and Balan, R. (2008). Frames for linear reconstruction without phase. *The 42nd Annual Conference on Information Sciences and Systems*, pages 721–726.
- [Bodmann and Paulsen, 2005] Bodmann, B. G. and Paulsen, V. I. (2005). Frames, graphs and erasures. *Linear Algebra and its Applications*, 404:118 – 146.
- [Casazza and Kovačević, 2003] Casazza, P. G. and Kovačević, J. (2003). Equal-norm tight frames with erasures. *Advances in Computational Mathematics*, 18(2):387–430.
- [Casazza and Kutyniok, 2008] Casazza, P. G. and Kutyniok, G. (2008). Robustness of fusion frames under erasures of subspaces and of local frame vectors. *Contemporary Mathematics*, 25:114–132.
- [Casazza et al., 2008] Casazza, P. G., Kutyniok, G., and Li, S. (2008). Fusion frames and distributed processing. *Applied and Computational Harmonic Analysis*, 25:114–132.
- [Cavazza et al., 2018] Cavazza, J., Morerio, P., Haefele, B., Lane, C., Murino, V., and Vidal, R. (2018). Dropout as a low-rank regularizer for matrix factorization. *Proceedings of the Twenty-First International Conference on Artificial Intelligence and Statistics*, 84:435–444.
- [Christensen, 2003] Christensen, O. (2003). An introduction to frames and riesz bases. *Birkhauser*.
- [Cotfas and Gazeau, 2010] Cotfas, N. and Gazeau, J. P. (2010). Finite tight frames and some applications. *Journal of Physics A: Mathematical and Theoretical*, 43(19):193001.
- [Donoho and Elad, 2003] Donoho, D. and Elad, M. (2003). Optimally sparse representation in general (nonorthogonal) dictionaries via ℓ^1 minimization. *Proc. Nat. Aca. Sci.*, 100(5):2197–2202.
- [Duarte-Carvajalino and Sapiro, 2009] Duarte-Carvajalino, J. M. and Sapiro, G. (2009). Learning to sense sparse signals: Simultaneous sensing matrix and sparsifying dictionary optimization. *IEEE Transactions on Image Processing*, 18(7):1395–1408.
- [Elad, 2007] Elad, M. (2007). Optimized projections for compressed sensing. *IEEE Transactions on Signal Processing*, 55(12):5695–5702.
- [Eldar, 2015] Eldar, Y. C. (2015). *Sampling Theory: Beyond Bandlimited Systems*. Cambridge University Press.
- [Goodfellow et al., 2016] Goodfellow, I., Bengio, Y., and Courville, A. (2016). *Deep Learning*. MIT Press.
- [Haikin and Zamir, 2016] Haikin, M. and Zamir, R. (2016). Analog coding of a source with erasures. In *2016 IEEE International Symposium on Information Theory (ISIT)*, pages 2074–2078.
- [Haikin et al., 2017] Haikin, M., Zamir, R., and Gavish, M. (2017). Random subsets of structured deterministic frames have MANOVA spectra. *Proceedings of the National Academy of Sciences*, 114(26):E5024–E5033.
- [Haikin et al., 2018] Haikin, M., Zamir, R., and Gavish, M. (2018). Frame moments and welch bound with erasures. *CoRR*, abs/1801.04548.
- [Han and Larson, 2000] Han, D. and Larson, D. R. (2000). Frames, bases and group representations. *American Mathematical Society*, 697.
- [Helmbold and Long, 2015] Helmbold, D. P. and Long, P. M. (2015). On the inductive bias of dropout. *Journal of Machine Learning Research*, 16:3403–3454.
- [Hinton et al., 2012a] Hinton, G., Deng, L., Yu, D., Dahl, G., Mohamed, A.-R., Jaitly, N., Senior, A., Vanhoucke, V., Nguyen, P., Sainath, T., and Kingbury, B. (2012a). Deep neural networks for acoustic modeling in speech recognition. *IEEE Signal Processing Magazine*, 29(6):82–97.

- [Hinton et al., 2012b] Hinton, G. E., Srivastava, N., Krizhevsky, A., Sutskever, I., and Salakhutdinov, R. R. (2012b). Improving neural networks by preventing co-adaptation of feature detectors. *NIPS*.
- [Ioffe and Szegedy, 2015] Ioffe, S. and Szegedy, C. (2015). Batch normalization: Accelerating deep network training by reducing internal covariate shift. In *Proceedings of the 32Nd International Conference on International Conference on Machine Learning - Volume 37, ICML’15*, pages 448–456. JMLR.org.
- [Kim, 2014] Kim, Y. (2014). Convolutional neural networks for sentence classification. In *EMNLP*, pages 1746–1751.
- [Kingma and Welling, 2013] Kingma, D. P. and Welling, M. (2013). Auto-encoding variational bayes. *CoRR*, abs/1312.6114.
- [Krizhevsky et al., 2012] Krizhevsky, A., Sutskever, I., and Hinton, G. E. (2012). Imagenet classification with deep convolutional neural networks. *Advances In Neural Information Processing Systems*, pages 1–9.
- [Krogh and Hertz, 1992] Krogh, A. and Hertz, J. A. (1992). A simple weight decay can improve generalization. In Moody, J. E., Hanson, S. J., and Lippmann, R. P., editors, *Advances in Neural Information Processing Systems 4*, pages 950–957. Morgan-Kaufmann.
- [Kukaka et al., 2017] Kukaka, J., Golkov, V., and Cremers, D. (2017). Regularization for deep learning: A taxonomy. In *ArXiv preprint*. href="https://arxiv.org/abs/1710.10686".
- [Larson and Scholze, 2015] Larson, D. and Scholze, S. (2015). Signal reconstruction from frame and sampling erasures. *Journal of Fourier Analysis and Applications*, 21(5):1146–1167.
- [LeCun et al., 1993] LeCun, Y., Simard, P. Y., and Pearlmutter, B. (1993). Automatic learning rate maximization by on-line estimation of the hessian’s eigenvectors. In Hanson, S. J., Cowan, J. D., and Giles, C. L., editors, *Advances in Neural Information Processing Systems 5*, pages 156–163. Morgan-Kaufmann.
- [Marcus et al., 1993] Marcus, M. P., Marcinkiewicz, M. A., and B., S. (1993). Building a large annotated corpus of english: The penn treebank. *Computational Linguistics*, 19(2):313–330.
- [Masci et al., 2011] Masci, J., Meier, U., Cireşan, D., and Schmidhuber, J. (2011). Stacked convolutional auto-encoders for hierarchical feature extraction. In Honkela, T., Duch, W., Girolami, M., and Kaski, S., editors, *Artificial Neural Networks and Machine Learning – ICANN 2011*, pages 52–59, Berlin, Heidelberg. Springer Berlin Heidelberg.
- [Mianjy et al., 2018] Mianjy, P., Arora, R., and Vidal, R. (2018). On the implicit bias of dropout. In *ICML*.
- [Neyshabur et al., 2015] Neyshabur, B., Tomioka, R., and Srebro, N. (2015). Norm-based capacity control in neural networks. In Grnwald, P., Hazan, E., and Kale, S., editors, *Proceedings of The 28th Conference on Learning Theory*, volume 40 of *Proceedings of Machine Learning Research*, pages 1376–1401, Paris, France. PMLR.
- [P. Baldi, 2014] P. Baldi, P. S. (2014). The dropout learning algorithm. *Artificial Intelligence*, 210:78–122.
- [Papayan et al., 2017] Papayan, V., Romano, Y., and Elad, M. (2017). Convolutional neural networks analyzed via convolutional sparse coding. *Journal of Machine Learning Research (JMLR)*, (18):1–52.
- [Papayan et al., 2018] Papayan, V., Romano, Y., Sulam, J., and Elad, M. (2018). Theoretical foundations of deep learning via sparse representations: A multilayer sparse model and its connection to convolutional neural networks. *IEEE Signal Processing Magazine*, 35(4):72–89.
- [Pu et al., 2016] Pu, Y., Gan, Z., Henao, R., Yuan, X., Li, C., Stevens, A., and Carin, L. (2016). Variational autoencoder for deep learning of images, labels and captions. In *Advances in Neural Information Processing Systems 29: Annual Conference on Neural Information Processing Systems 2016, December 5-10, 2016, Barcelona, Spain*, pages 2352–2360.
- [Ranzato et al., 2007] Ranzato, M., Huang, F. J., Boureau, Y., and LeCun, Y. (2007). Unsupervised learning of invariant feature hierarchies with applications to object recognition. In *2007 IEEE Conference on Computer Vision and Pattern Recognition*, pages 1–8.
- [Rifai et al., 2011] Rifai, S., Vincent, P., Muller, X., Glorot, X., and Bengio, Y. (2011). Contractive auto-encoders: Explicit invariance during feature extraction. In *International Conference on International Conference on Machine Learning (ICML)*, pages 833–840.
- [Rumelhart et al., 1986] Rumelhart, D. E., Hinton, G. E., and Williams, R. J. (1986). Parallel distributed processing: Explorations in the microstructure of cognition, vol. 1. chapter Learning Internal Representations by Error Propagation, pages 318–362. MIT Press, Cambridge, MA, USA.

- [Rupf and Massey, 2006] Rupf, M. and Massey, J. L. (2006). Optimum sequence multisets for synchronous code-division multiple-access channels. *IEEE Trans. Inf. Theor.*, 40(4):1261–1266.
- [Scardapane et al., 2017] Scardapane, S., Comminiello, D., Hussain, A., and Uncini, A. (2017). Group sparse regularization for deep neural networks. *Neurocomputing*, 241:81 – 89.
- [Simonian and Zisserman, 2015] Simonian, K. and Zisserman, A. (2015). Very deep convolutional networks for large-scale image recognition. *International Conference on Learning Representations (ICLR)*.
- [Sokolic et al., 2017] Sokolic, J., Giryès, R., Sapiro, G., and Rodrigues, M. R. D. (2017). Robust large margin deep neural networks. *IEEE Transactions on Signal Processing*, 65(16):4265–4280.
- [Srivastava et al., 2014] Srivastava, N., Hinton, G., Krizhevsky, A., Sutskever, I., and Salakhutdinov, R. (2014). Dropout: A simple way to prevent neural networks from overfitting. *Journal of Machine Learning Research*, 15. 1929–1958.
- [Vincent et al., 2008] Vincent, P., Larochelle, H., Bengio, Y., and Manzagol, P.-A. (2008). Extracting and composing robust features with denoising autoencoders. In *Proceedings of the 25th International Conference on Machine Learning, ICML '08*, pages 1096–1103, New York, NY, USA. ACM.
- [Vincent et al., 2010] Vincent, P., Larochelle, H., Lajoie, I., Bengio, Y., and Manzagol, P.-A. (2010). Stacked denoising autoencoders: Learning useful representations in a deep network with a local denoising criterion. *J. Mach. Learn. Res.*, 11:3371–3408.
- [Voulodimos et al., 2018] Voulodimos, A., Doulamis, N., Doulamis, A., and Protopapadakis, E. (2018). Deep learning for computer vision: A brief review. *Computational Intelligence and Neuroscience*.
- [Wachter, 1980] Wachter, K. W. (1980). The limiting empirical measure of multiple discriminant ratios. *Ann. Statist.*, 8(5):937–957.
- [Wager et al., 2014] Wager, S., Fithian, W., Wang, S., and Liang, P. S. (2014). Altitude training: Strong bounds for single-layer dropout. In *Advances in Neural Information Processing Systems (NIPS)*, pages 100–108.
- [Wager et al., 2013] Wager, S., Wang, S., and Liang, P. S. (2013). Dropout training as adaptive regularization. In *Advances in Neural Information Processing Systems (NIPS)*, pages 351–359.
- [Wan et al., 2013] Wan, L., Zeiler, M., Zhang, S., LeCun, Y., and Fergus, R. (2013). Regularization of neural networks using dropconnect. In *Proc. International Conference on Machine Learning (ICML'13)*.
- [Welch, 1974] Welch, L. (1974). Lower bounds on the maximum cross correlation of signals. *IEEE Transactions on Information theory*, 20.
- [Xiao et al., 2017] Xiao, H., Rasul, K., and Vollgraf, R. (2017). Fashion-mnist: a novel image dataset for benchmarking machine learning algorithms. *CoRR*, abs/1708.07747.
- [Zaremba et al., 2014] Zaremba, W., Sutskever, I., and Vinyals, O. (2014). Recurrent neural network regularization.
- [Zhang et al., 2015] Zhang, Y., Lee, J. D., and Jordan, M. I. (2015). 1-regularized neural networks are improperly learnable in polynomial time. *CoRR*, abs/1510.03528.
- [Zhang et al., 2016] Zhang, Y., Pezeshki, M., Brakel, P., Zhang, S., Laurent, C., Bengio, Y., and Courville, A. C. (2016). Towards end-to-end speech recognition with deep convolutional neural networks. In *Interspeech*, pages 410–414.